Rediscovering a Key Interface in Dye-Sensitized Solar Cells: Guanidinium and Iodine Competition for Binding Sites at the Dye/Electrolyte Surface

ARTICLE *in* JOURNAL OF THE AMERICAN CHEMICAL SOCIETY · MAY 2014

Impact Factor: 12.11 · DOI: 10.1021/ja411560s · Source: PubMed

8 AUTHORS, INCLUDING:

Piers R. F. Barnes
Imperial College London
79 PUBLICATIONS **3,473** CITATIONS
SEE PROFILE

P. Lund
Aalto University
253 PUBLICATIONS **3,537** CITATIONS
SEE PROFILE

Muhammad Imran Asghar
Aalto University
34 PUBLICATIONS **351** CITATIONS
SEE PROFILE

JACS
JOURNAL OF THE AMERICAN CHEMICAL SOCIETY

Article

pubs.acs.org/JACS

Rediscovering a Key Interface in Dye-Sensitized Solar Cells: Guanidinium and Iodine Competition for Binding Sites at the Dye/Electrolyte Surface

Xavier A. Jeanbourquin,[†,§] Xiaoe Li,[†] ChunHung Law,[†] Piers R.F. Barnes,[‡] Robin Humphry-Baker,[§] Peter Lund,[∥] Muhammad I. Asghar,[∥] and Brian C. O'Regan*[,†]

[†]Chemistry Department and [‡]Physics Department, Imperial College London, 1 Exhibition Way, London SW7 2AZ, United Kingdom
[§]Laboratoire de Photonique et Interfaces, Ecole Polytechnique Federal Lausanne, CH1015 Lausanne, Switzerland
[∥]Department of Applied Phyics, Alto University, P.O. Box 15100, FI-00076 Aalto, Finland

Supporting Information

ABSTRACT: We propose a new mechanism by which the common electrolyte additive guanidinium thiocyanate (GdmSCN) improves efficiency in dye-sensitized solar cells (DSSCs). We demonstrate that binding of Gdm^+ to TiO_2 is weak and does not passivate recombination sites on the TiO_2 surface as has been previously claimed. Instead, we show that Gdm^+ binds strongly to the N719 and D131 dyes and probably to many similar compounds. The binding of Gdm^+ competes with iodine binding to the same molecule, reducing the surface concentration of dye−I_2 complexes. This in turn reduces the electron/iodine recombination rate constant, which increases the collection efficiency and thus the photocurrent. We further observe that $GdmNO_3$ can increase efficiency more than the current Gdm^+ source, GdmSCN, at least in some DSSCs. Overall, the results point to an improved paradigm for DSSC operation and development. The TiO_2/electrolyte surface has long been held to be the key interface in DSSCs. We now assert that the dye layer/electrolyte interaction is at least, and probably more, important.

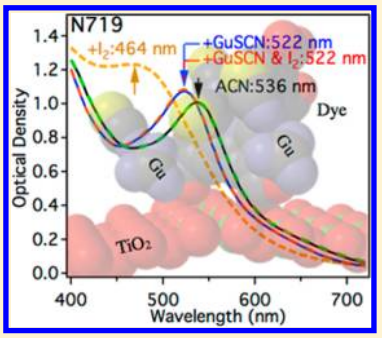

INTRODUCTION

Dye-sensitized solar cells (DSSCs) grew out of the semiconductor photoelectrochemistry community in the 1960s and 1970s.[1−6] Because of this origin, early hypotheses about DSSC internal workings were drawn from the experience of that community. For example, central concepts in semiconductor electrochemistry include the chemical "passivation" of surface sites to reduce recombination and the binding of "potential determining ions" to control the energy position of the band edge. This focus on species binding to the semiconductor surface was inherited by the DSSC community and has remained a central paradigm for the ensuing 30+ years of research. For example, virtually all new additives or treatments that increased or decreased current and/or voltage have been assumed to bind to the TiO_2, and this binding has been assumed to be the basis of the observed effects.[7−14] It appears to have escaped notice, including by the corresponding author of this article, that the dye layer could well have a much richer "binding chemistry" than the TiO_2 surface. For example, N719, the most common dye, has pendant sulfur groups, π-system electrons, and one or more carboxylates that are not bound to the TiO_2. Some years ago, we and others detected that iodine binds strongly to many dye molecules, and that this binding increases the recombination rate constant in DSSC cells.[15−20] These results suggested that recombination involves the direct reduction of molecular iodine (I_2) rather than tri-iodide (I_3^-). We have recently confirmed this suggestion by concentration studies of the recombination rate constant.[21] Subsequently, we found that the presence of the dye layer by itself does not block recombination and can actually increase it, indicating (but not proving) that most recombination to the electrolyte is catalyzed by the dye.[22,23] In this article, we show that guanidinium, $C(NH_2)_3^+$, a common electrolyte ingredient, binds to both Ru-centered dyes such as N719 and to typical organic dye molecules such as D131. We find that the binding of guanidinium (Gdm^+) to N719 competes with the binding of iodine, and that this in turn influences the overall recombination rate constant. In our view, this now proves that most recombination occurs via "dye-based catalysis" in standard DSSCs. Moreover, this has caused us to revise our opinions about the importance of the TiO_2/electrolyte interface. We now suggest that the dye/electrolyte "interface" accounts for many of the positive and negative effects of electrolyte ingredients. Lack of focus on the dye/electrolyte interaction may have slowed DSSC progress considerably over the last decades. For example, it now seems that a 10 year delay occurred in the development of cobalt-based electrolytes because it was not appreciated that cobalt complexes might bind to the COO^- of the N719 dye.[15] We hope an increased appreciation for dye/electrolyte interactions will help accelerate DSSC research in the future.

Received: November 22, 2013
Published: May 2, 2014

   dx.doi.org/10.1021/ja411560s | J. Am. Chem. Soc. 2014, 136, 7286−7294

Many electrolyte additives in DSSCs, such as *tert*-butylpyridine (TBP), lithium iodide (LiI), or guanidinium thiocyanate (GdmSCN) have been found, which improve power conversion efficiency (PCE).[24] GdmSCN, which is the topic of this work, is frequently used in laboratory and commercial electrolytes. A survey of the literature shows, however, that the working mechanism and even the exact effect remain unclear. GdmSCN was first introduced into the dye solution by Grätzel and co-workers in 2003.[25] At that time, they speculated that the beneficial effect stemmed from an improvement in self-assembly of the dye layer. Following that, it was introduced as an additive in the electrolyte where it has been said to give a noticeable increase in the PCE.[26] GdmSCN is also frequently used as a replacement for LiI in electrolytes designed for thermal stability.[27] Its effect was investigated for the first time in 2006 by Kopidakis et al.[14] They reported that addition of GdmSCN resulted in a slight increase in the voltage at open circuit (V_{oc}) and little change in J_{sc}. From kinetic measurements, they reported a reduction in the recombination rate. However, the V_{oc} increase expected from this reduction was offset by a downshift in the conduction band potential (V_{cb}) of the TiO_2. On the basis of the results, they proposed a model in which Gdm^+ was hypothesized to adsorb to the TiO_2. The adsorption was suggested to both passivate recombination and lower the V_{cb} due to the positive charge. In 2009, Zhang and co-workers reported that addition of GdmSCN significantly increased the short circuit current (J_{sc}) and slightly increased the V_{oc}. Following the suggestions of Kopidakis et al., they assumed that the effect on the J_{sc} was caused by the higher driving force for electron injection due to the downshift in V_{cb}. The most recent work on the GdmSCN additive was published by Kloo and co-workers in 2010.[28] In their devices, increase in J_{sc} was again observed, but there was no change in V_{oc}. In opposition to the assumptions of the two previous articles, Kloo et al. could not find evidence that Gdm^+ adsorbed to the TiO_2 using Raman spectroscopy of TiO_2 particles in Gdm^+-containing solutions. We present here a thorough reinvestigation of the effect of GdmSCN in iodide/iodine-based DSSCs using transient analysis of kinetics and UV−vis binding assays. We investigate three different dyes and cells with bare TiO_2. Taken together, the data indicate a revision of the mechanism of GdmSCN function, as outlined in the first paragraph.

EXPERIMENTAL SECTION

The devices were fabricated according to the following procedure. Fluorine-doped tin oxide (FTO) conductive glass (Pilkington) was washed with soap and deionized water and then rinsed with isopropyl alcohol (IPA). The plate was then heated to 450 °C for 30 min and cooled to room temperature (RT). TiO_2 paste (Dyesol, DSL 18-NRT) was spread over the FTO glass using the so-called doctor blading technique. The plate was then heated again at 450 °C for 30 min, resulting in a transparent TiO_2 film approximately 7 μm thick. The mesoporous film was placed in a bath of 30 mM $TiCl_4$−THF complex (Sigma-Aldrich) in water at 70 °C for 30 min and then rinsed with deionized water and IPA prior to heating again at 450 °C for 30 min. Once cooled to RT, the plate was cut to device size (1.6 × 2.5 cm^2). The area covered by the mesoporous film was reduced to 1 × 1 cm^2 by scraping off any excess (1 cm^2 active area). The films were heated back to 450 °C for 30 min, cooled to around 120 °C, and placed in a dye solution. Dye sensitization was carried out overnight in a solution containing 0.3 mM N719 (Dyesol) or Z995 (EPFL) in a mixed solvent (1:1 vol) of *tert*-butyl alcohol (TBA) (Alfa Aesar, 95% anhydrous) and acetonitrile (ACN) (Sigma-Aldrich) overnight. D131 sensitization was performed in a solution of 0.0625 mM D131 (Mitsubishi) and 0.25 mM chenodoxycholic acid (Cheno) (Sigma-Aldrich) in TBA/ACN (1:1 vol) for 3 h. The sensitized films were rinsed in ACN prior to device fabrication. For the counter electrode, a FTO conductive glass was cut to device size. Two holes were drilled at opposite corners of a centered 1 × 1 cm^2 area. The pieces of glass were then cleaned with soap and water, rinsed with IPA, and heated to 450 °C for 30 min. Once cooled to RT, a solution of H_2PtCl_6 (5 mM) in IPA was deposited on the surface. The glass was then heated at 400 °C for 30 min and kept at 120 °C until device assembly. A Surlyn polymer film from Dupont was used to seal the working electrode and the counter electrode together. Sealing was performed at 120 °C for ∼1 min. The electrolyte was injected into one of the two holes. The holes were sealed using a glass microscope coverslip and Surlyn. A tin−lead alloy was melted on the contact of both electrodes. In the case of the cells containing TiO_2 films without dye, it was found that more reproducible results could be obtained if fresh electrolyte was flushed through the cell three times before sealing the holes.[29] For each flushing, we fill the cell (∼2 μL) and then remove the electrolyte by vacuum. We presume this allowed the electrolyte components to equilibrate with the TiO_2 surface. The electrolyte flushing is required due to the small volume of electrolyte (∼2 $\mu L/cm^2$) relative to the large internal surface area of the TiO_2 film (∼1000 cm^2).

If not specified otherwise, the electrolyte consists of 0.8 M 1-methyl-3-*n*-propylimidazolium iodide (PMII) (Alfa Aesar, 98%), 0.05 M I_2 (Sigma-Aldrich, 99+ %), 0.5 M *tert*-butylpyridine (Sigma-Aldrich, 96%) in methoxypropionitrile (MPN) (Sigma-Aldrich). The GdmSCN additive (Fluka) was used at a concentration of 0.1 M. All measurements were performed at RT and in air unless indicated otherwise. At least two identical samples were fabricated for every test.

Current/voltage ($J-V$) measurements were performed under simulated 1 sun illumination (AM 1.5) using a 150 W xenon lamp with an AM 1.5 global filter. Calibration was done with a silicon photodiode before measurements. For the measurements, the applied voltage was swept from 0 to 1 V and then back to −1 V before finishing at 0 V. The data were recorded using a Keithley 2400 sourcemeter. Transient measurements were performed using the IC designed and built TRACER system.[30] TRACER uses five 1 W red-light-emitting diodes (LED) controlled by a fast solid-state switch to induce a pump pulse, as described elsewhere.[31] Bias light was provided by an array of 10 white LEDs.[16,32] Injected excess charge density in the dark was measured by integrating the current pulse after the cell had been rapidly switched from a given voltage to short circuit. To achieve this MOSFET, switches were used to disconnect the cell from the voltage source and at the same moment (synchronicity <1 μs) switch the cell to short circuit across a small measuring resistor (∼2 Ohms).[33]

Incident photon to current conversion efficiency (IPCE) measurements were done using a 100 W tungsten halogen lamp coupled to a monochromator with computer-controlled stepper motor. Calibration of the incident light was performed using a UV-enhanced silicon photodiode. A 590 nm long-pass filter was used for wavelengths longer than 620 nm to remove the light resulting from second-order diffraction. All the measurements were performed under ∼10% sun bias light provided by an array of white LEDs. The samples were placed either with the working electrode (front) or with the counter electrode (back) facing the beam. A Keithley 2400 sourcemeter was used to record the data. Analysis of the front and back IPCE data to obtain the collection efficiency was made using a model described elsewhere.[34]

The experimental procedure for the binding measurements was performed as reported elsewhere.[18] The films consisted of N719, Z995, or D131 adsorbed on a transparent TiO_2 mesoporous film (4 μm thick). Dye sensitization of the films was carried out as reported for the device fabrication. The films were rinsed in ACN prior to incubation in various concentrations of the molecule under test. Binding measurements of iodine and guanidinium were performed in solutions of, respectively, 0.35 mM and 0.1 M in ACN. The films were left in the solution for 30 min prior to measurement of the absorption spectrum in order to reach equilibrium. Absorption spectra were recorded using a Thermo Genesys 10 UV−vis spectrophotometer.

The samples for Raman spectroscopy were made in a similar fashion to the full cells described above. The "counter electrodes" in this case

were 1 mm microscope slides. Illumination for the Raman spectra was carried out through the microscope slide. Illumination wavelength was 531 nm.

RESULTS AND DISCUSSION

Figure 1 contains representative $J-V$ curves for cells with and without the GdmSCN additive. Table 1 gives the average

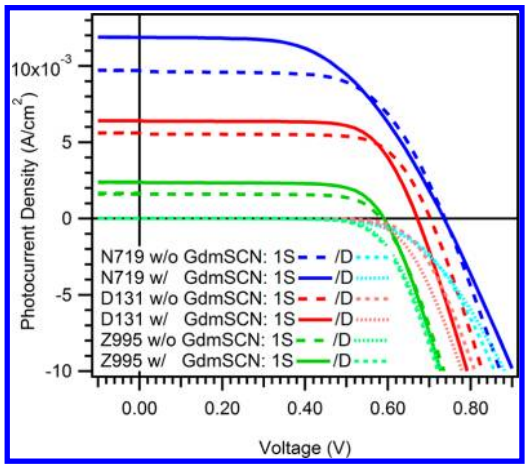

Figure 1. Typical $J-V$ curves measured under 1 sun (1S) and in the dark (D) for N719, D131, and Z995 DSSCs with and without 0.1 M GdmSCN.

Table 1. Average $J-V$ Results at 1 sun for DSSCs Sensitized with N719, D131, and Z995[a]

dye	additive	J_{sc} (mA/cm^2)	V_{oc} (volt)	FF	η (%)
N719	no GdmSCN	9.83	0.74	0.63	4.57
N719	0.1 M GdmSCN	11.77	0.74	0.56	4.84
D131	no GdmSCN	6.00	0.71	0.73	3.05
D131	0.1 M GdmSCN	6.29	0.68	0.73	3.12
Z995	no GdmSCN	1.78	0.59	0.75	0.77
Z995	0.1 M GdmSCN	2.40	0.60	0.76	1.10

[a]The electrolyte consists of 0.8 M PMII, 0.5 M TBP, and 0.05 M I_2 in MPN, with or without 0.1 M GdmSCN as specified. The fill factor (FF) variation is likely spurious, due to the small sample and variation in cell series resistance. Values are average of at least two cells.

results of at least two cells for each treatment. The average effect of the GdmSCN additive on our N719 cells is an improvement in J_{sc} of ~20%, with little change in the V_{oc}. Our data thus agree with the results obtained by Kloo and co-workers.[28] Supporting Information Table S1c shows the effects of variation of the GdmSCN concentration from 10 to 200 mM. We find a broad maximum in efficiency around 100 mM. In contrast, for the cells containing the organic dye D131, the J_{sc} is enhanced by ~5% and the V_{oc} is decreased by ~4%. Lastly, for cells containing Z995, an N719-like dye not containing thiocyanates (Scheme 1), the J_{sc} was increased by ~35% with essentially no change in V_{oc}. Thus, the main effect of GdmSCN, in our experiments, is an increase in J_{sc}. Increased J_{sc} means either an increase in the charge separation efficiency (i.e., electron injection) or an increase in the charge collection efficiency. (We are assuming small or no change in light harvesting.) To test for the contribution of charge collection efficiency, we made a series of cells with differing iodine (acceptor) concentrations in the electrolyte (Table 2). The J_{sc} results in Table 2 show that photocurrent goes down with increasing iodine, but the relative improvement in photocurrent from GdmSCN goes up. This is consistent with GdmSCN causing an increase in collection efficiency. We have also measured the collection efficiency using the comparison of spectral response (IPCE) for front and back illumination. The relative increase in collection efficiency from the IPCE measurements is roughly consistent with the relative increase in J_{sc} for the no GdmSCN and GdmSCN cells. The results in Table 2 indicate that much of the improvement caused by GdmSCN can be attributed to increased collection efficiency. The results do not preclude some increase in charge separation, but it is probably not the main effect as has been postulated in earlier reports.[35]

Taken together, the results in Table 1 show that the effect of the GdmSCN additive varies with different dyes used. This calls into question the hypothesis that the effects of GdmSCN are caused by Gdm^+ adsorption to TiO_2. To examine this last question, we first wished to verify that the effects of GdmSCN were indeed due to Gdm^+ alone and not related to SCN^- or the combination of the two. Gdm^+ has previously been indicated to be the sole actor in ref 28. As our films and electrolytes are slightly different, we again compared the effects of GdmSCN, $GdmNO_3$, and $GdmClO_4$ (Table S1). Our results corroborate those of Kloo et al; we also find that Gdm^+ is responsible for the beneficial effect. However, in our limited number of tests, the additive $GdmNO_3$ in fact performed better than GdmSCN, due to an improvement in V_{oc} and fill factor. This shows that the anion is not simply an innocent bystander. If further work verifies the advantage of $GdmNO_3$, and it is found to be stable, it might be a valuable replacement for GdmSCN.

We turn to the question of the mechanism for the beneficial effect of Gdm^+. If, as previously thought, the adsorption of Gdm^+ to the surface of TiO_2 reduces electron/electrolyte recombination, then one should be able to observe this effect

Scheme 1. Structures of the Different Dyes Used in This Work (Left to Right N719, Z995, and D131)

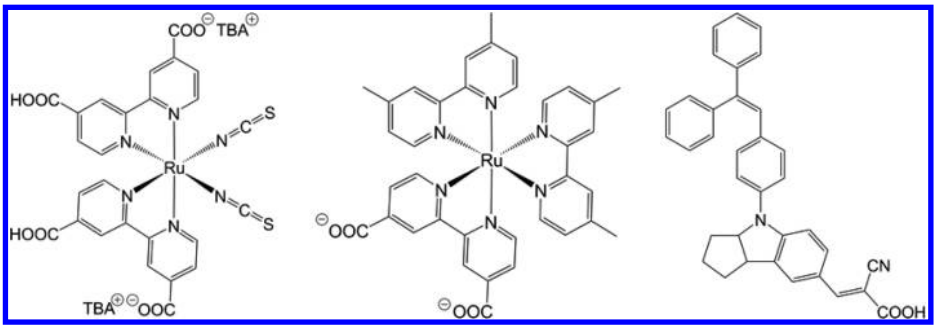

dx.doi.org/10.1021/ja411560s | J. Am. Chem. Soc. 2014, 136, 7286−7294

Table 2. $J-V$ Results for N719 Cells with Differing Iodine Concentrations and with and without 0.1 M GdmSCN in the Electrolyte

	J_{sc} (mA/cm^2)	V_{oc} (volt)	FF	η (%)	ratio of J_{sc} w/wo GdmSCN	ratio of η_{col} w/wo GdmSCN
10 mM I_2 (without GdmSCN)	6.3	0.72	0.62	2.83	1.17	1.15
10 mM I_2 (with GdmSCN)	7.4	0.72	0.63	3.30		
50 mM I_2 (without GdmSCN)	6.0	0.69	0.71	2.91	1.22	1.13
50 mM I_2 (with GdmSCN)	7.3	0.68	0.68	3.36		
200 mM I_2 (without GdmSCN)	5.6	0.64	0.74	2.68	1.23	1.21
200 mM I_2 (with GdmSCN)	6.9	0.64	0.72	3.20		

[a]All $J-V$ curves were taken with ~0.6 sun intensity because the 10 mM I_2 cells were diffusion-limited above that level. Last column is the increase in collection efficiency as determined from IPCE analysis.

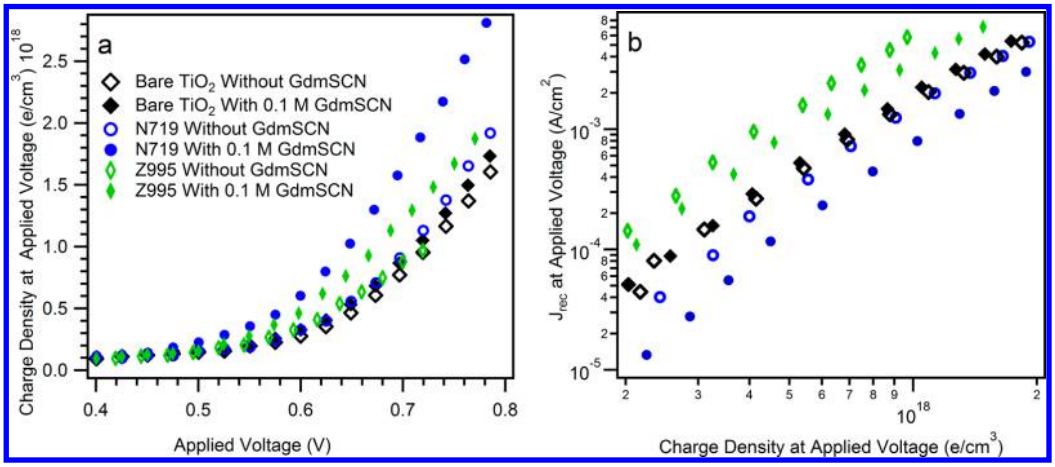

Figure 2. (a) Charge density vs applied forward bias in the dark for bare TiO_2 films in the iodide/iodine electrolyte and for typical DSSCs sensitized with N719 and Z995. (b) Dark current (recombination flux) for a given applied voltage vs charge density at the same voltage for bare TiO_2 and typical N719 and Z995 DSSCs.

on TiO_2 films without adsorbed dye. We have previously used the "charge extraction from applied voltage in the dark" measurement to investigate the effect of dye coverage on recombination.[22] The technique allows simultaneous determination of conduction band edge shifts and comparison of dark current for a given charge density in the TiO_2. This latter comparison allows one to see real changes in recombination rate constant by removing the effect of conduction band shifts on dark current. This is because, specifically for DSSCs, the interfacial electron transfer event giving rise to dark current is identical to the "recombination" of photoinjected charges under light. In both case, the current is the reduction of the electrolyte by electrons from the TiO_2.

Figure 2a shows the charge density versus applied voltage in the dark for cells with and without GdmSCN in the electrolyte. If the overall trap density distribution is not changed, shifts to the left in Figure 2a correspond to downshifts in the conduction band potential (see Figure S6a). For the cells containing TiO_2 films without dye ("bare TiO_2"), the average downshift caused by GdmSCN is 12 mV. This value is the result of averaging four cells for each condition. The graph shows a specific pair of cells that show the average shift. The small shift (relative to ≥100 mV for 0.1 M LiI)[36,37] indicates that, though there may be some adsorption of Gdm^+ to the TiO_2, in this electrolyte the adsorption is rather weak and the coverage is low.

Figure 2b shows the recombination flux (i.e., the dark current) versus charge for the same cells shown in Figure 2a. For the TiO_2 films without dye, there is no shift toward lower recombination in the Gdm^+-containing electrolyte. Data from three additional cells fall on exactly the same line and have been omitted for clarity. This result indicates that the Gdm^+ adsorbed to the TiO_2 surface does not increase or decrease electron transfer from TiO_2 to the iodine/iodide electrolyte.

Figure 2a also compares typical charge density versus applied voltage for cells with TiO_2 films dyed with N719 or Z995. The apparent downshift in the conduction band resulting from GdmSCN addition is 30 mV for Z995 and 60 mV for N719. The fact that the shift is 3 and 6 times larger, respectively, for the dyed TiO_2 films suggests that Gdm^+ is binding strongly to the dye molecules at the TiO_2 surface. Gdm^+ bound to the dye will also increase the net positive charge between the electrolyte and TiO_2 surface and thus shift the conduction band positive with respect to the electrolyte. Recall also that the fraction of free TiO_2 surface available in the dyed films should be significantly smaller than that in the bare TiO_2. Thus, in the dyed films, the contribution of Gdm^+ bound directly to TiO_2 appears to be very small.

Figure 2b compares the recombination versus charge data for cells containing TiO_2 films dyed with N719 or Z995. It is apparent the Gdm^+ does reduce recombination flux for cells containing each of these dyes. By process of elimination, the reduction of recombination must involve an interaction of the Gdm^+ and the dye. We note that the reduced recombination cannot be caused by Gdm^+ interaction with the redox species in solution or it would also be seen in the cells without dye. The cells in Figure 2b were not specifically constructed to test the difference in recombination between cells with and without dye. Nonetheless, the general result is in agreement with our earlier finding that N719 does block recombination somewhat,

dx.doi.org/10.1021/ja411560s | J. Am. Chem. Soc. 2014, 136, 7286−7294

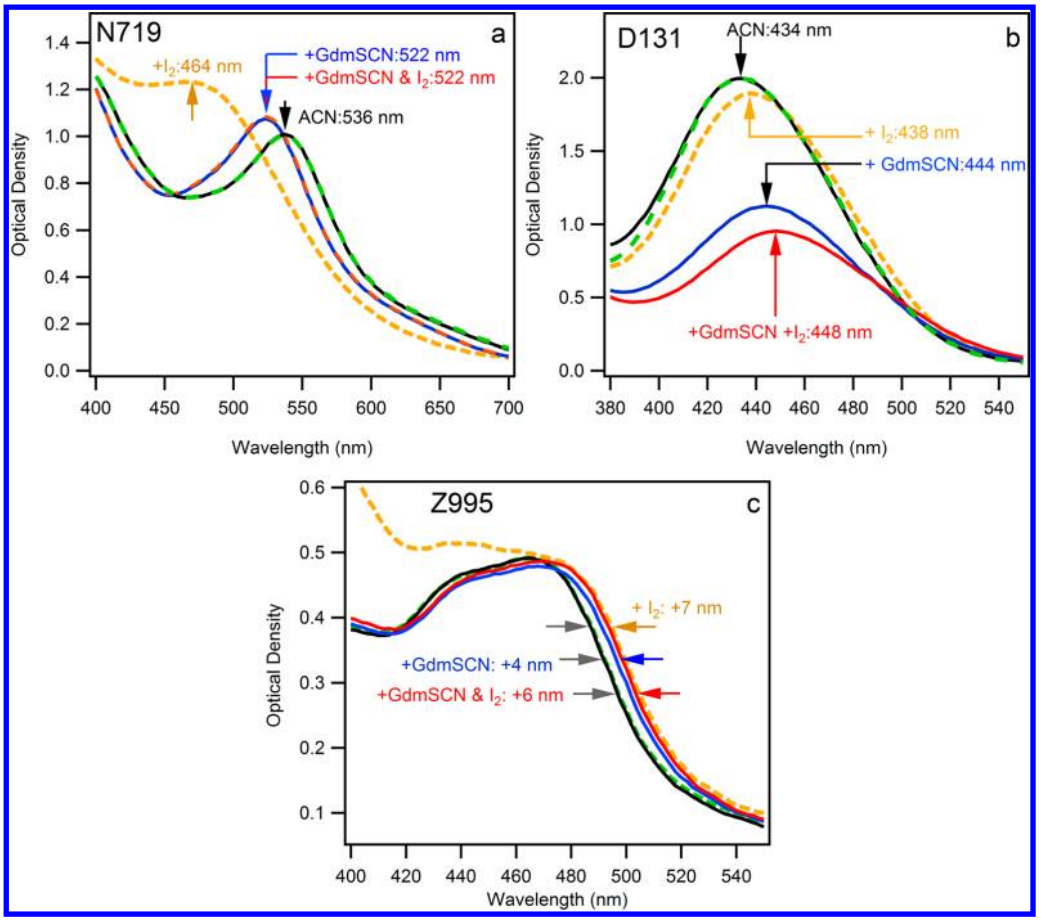

Figure 3. UV–vis spectrum of (a) N719/TiO_2 films, (b) D131/TiO_2 films, and (c) Z995/TiO_2 films. Films were 4 μm thick in this experiment to avoid saturation at the peak. In each case, one film was placed in ACN and then in 0.35 mM I_2 in ACN (green and orange dashed lines, respectively), while another film was placed in ACN, then in 0.1 M GdmSCN in ACN, and finally in 0.35 mM I_2 and 0.1 M GdmSCN in ACN (black, blue, and red solid lines, respectively; the red line in (a) is dashed for a better clarity). The arrows indicate the peaks maximum in (a) and (b). Arrows in (c) directly indicate shifts between the film in pure ACN and in the presence of GdmSCN or/and I_2. Small differences in the initial optical density of the two films in each case have been removed by normalization.

relative to a bare TiO_2 film.[22] Here we find that the difference between the bare and N719 dyed film is considerably increased when GdmSCN is present. On the other hand, Z995 cells without GdmSCN show significantly more recombination (for a given charge) than does bare TiO_2. This is consistent with the much lower V_{oc} for Z995 cells without GdmSCN, even though the conduction band edge of these cells appears to be about the same energy as that in bare TiO_2 and N719 without GdmSCN (Figure 2a). The observed ~6-fold increase in recombination in Figure 2b would give a about half the 140 mV decrease in voltage between N719 and Z995. The other half is due to the decreased light harvesting of Z995 relative N719 (see Figure 3c).

Direct evidence of interaction between Gdm^+ and dyes can be obtained from the UV–vis spectra in the presence of GdmSCN. Figure 3 shows the absorption spectra of TiO_2/dye films immersed in acetonitrile with and without GdmSCN and also with or without iodine. In the case of N719 (Figure 3a), the addition of GdmSCN results in a blue shift of ~14 nm. The addition of iodine gives a larger blue shift of ~58 nm, as we have previously shown.[17,18] There is also an increase in the peak absorption in both cases. Figure S1 shows that the addition of TBASCN does not cause a spectral shift of N719, indicating that SCN^- is not causing the shifts observed in Figure 3. We also measured the spectrum of N719 in solution, with and without GdmSCN. Approximately, the same blue shift occurs in solution as on the surface, showing that the spectral shift is not due to GdmSCN binding to TiO_2 adjacent to the dye (Figure S2a). Figure 3a also shows that, after immersion in Gdm^+-containing ACN, a subsequent immersion in iodine and Gdm^+-containing solution gives no additional shift. This result indicates that Gdm^+ can inhibit the binding of iodine to the dye. The order of Gdm^+ and I_2 exposure is not important; the same result was obtained when iodine was applied first, followed by addition of Gdm^+ (Figure S2b). Similar UV–vis spectral shifts are obtained when the experiment is done with iodine and $GdmClO_4$ instead of GdmSCN, again confirming that the iodine binding inhibition is due to Gdm^+ and not SCN^- (Figure S3). In previous work, we have shown that iodine binds to the thiocyanate groups of N719,[18] and we assume that Gdm^+ binds at or near the same site. The much lower concentration of iodine used in Figure 3 is intended to reflect the much lower concentration of free iodine (i.e., that not bound in tri-iodide) present in the cell electrolyte. We note that the blue shift and increased absorption seen in Figure 3a does not increase the total flux of absorbed photons (light harvesting) and thus cannot by itself be responsible for the increase in J_{sc} in Table 1.

In the case of TiO_2/D131 films, we find that the immersion in a few milliliters of 0.1 M GdmSCN in ACN results in

dx.doi.org/10.1021/ja411560s | J. Am. Chem. Soc. 2014, 136, 7286–7294

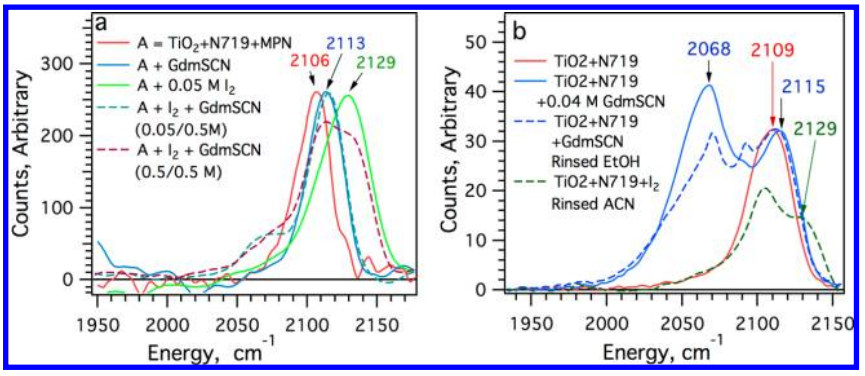

Figure 4. Vibrational spectroscopy of TiO_2/N719 with and without GdmSCN. (a) Raman spectra measured on TiO_2 particles sensitized with N719 dye, immersed in various solutions. (b) ATR-FTIR spectra taken with a diamond anvil cell. The first three spectra were taken sequentially on the same TiO_2/N719 film using a flow cell. Spectra have been normalized, by ≤10% at the ∼2100 peak. The spectrum of TiO_2/N719 + iodine is taken from our previous report on dye−iodine binding.[18] Wider energy windows are shown in Figure S15a,b.

significant desorption of the dye from the TiO_2 surface. After 30 min, the dissolved dye is clearly visible in the solution. Despite the decrease in absorption, we can observe a ∼10 nm red shift in the dye absorption in the GdmSCN solution. A red shift caused by binding an acceptor indicates overall stabilization of the LUMO relative to the HOMO. The D131 dye (shown in Scheme 1) is said to have the LUMO orbitals concentrated at the cyanoacrylate end of the molecule.[38,39] We presume that the Gdm^+ binding occurs somewhere in this area. Consistent with this, binding of Gdm^+ at or near the attachment group of the dye will balance the charge of the COO^-, reducing the electrostatic attraction to the TiO_2, thus explaining the desorption of the dye in GdmSCN solution. For the TiO_2/D131 films, immersion in 0.35 mM I_2 causes an ∼4 nm red shift in the spectrum (Figure 3b). Iodine solution does not cause significant desorption of D131, possibly because it adds no net positive charge or because its binding site is further away from the anchoring group. Immersion in GdmSCN and iodine solution after GdmSCN alone causes a further red shift of 4 nm. The shift caused by iodine and GdmSCN appears to be additive in the case of D131, suggesting that there is little competition between the binding of Gdm^+ and I_2 to the dye. This latter point will be important in further discussion below. We note that the effect of dye desorption will be limited in the actual solar cell due to the ∼500-fold smaller volume of electrolyte present for the same surface area of TiO_2. The level of desorption in the actual solar cell does not reduce the J_{sc} (Table 1), but it cannot be excluded that it limits to some extent the increase in J_{sc} seen or that it may degrade the cell over time.

In the case of TiO_2/Z995 films (Figure 3c), the spectral shifts are somewhat obscured by the broad double peak and by the lack of change in peak height. Nonetheless, there is a red shift of ∼4 nm in the GdmSCN solution and a red shift of ∼7 nm in the iodine solution. These shifts are best observed along the right edge of the absorption peak. Relative to N719, the shifts are reversed in direction and much smaller in magnitude. This provides further evidence that the blue shifts caused by the iodine and Gdm^+ in N719 are both due to a binding at the thiocyanate group. The removal of the thiocyanate being the major difference between the two dyes. Subsequent immersion of the Gdm^+-exposed film in GdmSCN + iodine solution results in an intermediate shift of about ∼6 nm. This suggests that some competition between the two species may be occurring. We correct here our statement in an earlier publication that Z995 does not bind iodine. In the previous work, we were viewing Z995 only in the light of the lack of blue shift due to the removal of the thiocyanate groups.[18] Titration of the red shift of Z995 gives a similar iodine binding coefficient to those found for N719 and C106 (Figure S4). We also tested for Z995 binding to I_3^-. No spectral shift is observed in 0.35 mM I_3^- in ACN (Figure S5).

We have also confirmed a specific interaction between Gdm^+ and N719 using Raman and FTIR spectroscopy. Figure 4a shows the variation in the Raman peak near 2100 cm^{-1}, which corresponds to the C═N vibration of the thiocyanate in the N719 dye.[40] For the blank sample, we have used TiO_2 with N719, immersed in neat MPN solvent (Figure 4a, red line). The SCN^- peak appears at 2106 cm^{-1}, in agreement with a previous report showing 2108 cm^{-1}.[40] When iodine (0.05 M) is added, this peak shifts to higher energy by about 20 cm^{-1} (Figure 4a, green line), in agreement with our earlier measurements using FTIR.[18] Alternatively, when GdmSCN (0.5 M) is added by itself, there is a smaller shift of ∼7 cm^{-1} (blue line). This corresponds to the weaker blue shift for GdmSCN in the spectrum in Figure 3a. When the TiO_2/N719 film is exposed to MPN with 0.05 M I_2 and 0.5 M GdmSCN, the shift is identical to that with GdmSCN alone (blue dashed line). However, if equimolar I_2 and GdmSCN are used, both Gdm^+-bound and I_2-bound SCN^- peaks result (purple dashed line). We note that the relatively equal peaks using equimolar Gdm^+ and I_2 concentrations actually indicate that Gdm^+ binds more weakly than I_2. This is because the added SCN^- will reduce the effective iodine concentration due to iodine/thiocyanate binding. (We note that the SCN^- will not cause a large change in free iodine in the full electrolyte because virtually all the iodine already exists as I_3^-. Assuming about the same binding for I_2 to I^- and SCN^-, the addition of 0.5 M SCN^- to 1 M I^- containing solution will only reduce the remaining free iodine by 33%.)

Figure 4b shows similar results measured by ATR-FTIR. In this case, the exposure of a TiO_2/N719 film to 0.04 M GdmSCN in EtOH results in a 6 cm^{-1} shift to higher energy (Figure 4b, blue line). Another peak appears at 2068 cm^{-1}, which is due to the SCN^- dissolved in the ethanol. This is verified by the reference spectrum of GdmSCN in ethanol (blue dashed line). There is also a characteristic peak for Gdm^+ at 1668 cm^{-1} (see Figure S15b). After being rinsed in flowing ethanol, the SCN^- peak at 2115 cm^{-1} does not shift back to 2109 cm^{-1}, indicating that Gdm^+ is still bound. The Gdm^+ peak

dx.doi.org/10.1021/ja411560s | J. Am. Chem. Soc. 2014, 136, 7286−7294

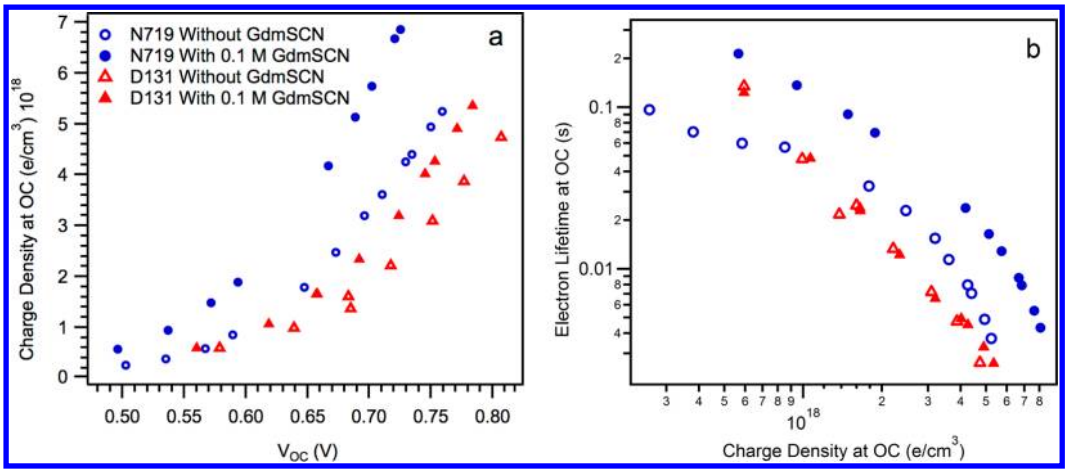

Figure 5. (a) Charge density at open circuit (from charge extraction) vs the corresponding V_{oc} at different light intensities. (b) Electron lifetime at open circuit (from photovoltage transients) vs the charge density at open circuit.

at 1668 is also not noticeably decreased (Figure S15b). After exposure of a TiO_2/N719 film to iodine (30 mM), followed by a rinse with acetonitrile, there are two peaks, one shifted by about 20 cm^{-1} to 2129 cm^{-1}. This is the same shift observed in the Raman spectrum. The existence of two peaks in FTIR, compared the single peak observed in Raman, is because the film in Figure 4b was rinsed in neat acetonitrile before the spectrum was collected. This removed some of the bound iodine, but not all.

Taken together, the data in Figures 2, 3, and 4 indicate strongly that Gdm^+ binds to dye molecules and that the improvement in the $J-V$ curve of the cells is largely due to this binding. Also, exposure to GdmSCN does not seem to decrease recombination from bare TiO_2 films. For completeness, however, we have also checked for GdmSCN binding to bare TiO_2 films, using FTIR (Figure S16). We find that, after exposure to GdmSCN, a rinse in dimethylimidazolium iodide (DMMI) electrolyte does not remove the signal from Gdm^+. This indicates some specific adsorption of Gdm^+ on TiO_2. However, a rinse in LiTFSI electrolyte fully removes the Gdm^+. We conclude that the binding of Gdm^+ to TiO_2 is significantly weaker than that of Li^+, explaining the small shift in the conduction band edge in Figure 2a. The equivalent concentration of Li^+ would cause a downshift of more than 100 mV.

We now return to the evidence that the binding of Gdm^+ to the dye reduces the recombination rate. Figure 2b shows that, for N719 and Z995, there is a decrease in recombination flux for the same charge density, and that no such change occurs when the dye is not present. In Figure 5, we present results of charge extraction from V_{oc} and small perturbation photovoltage transients at V_{oc}. Consistent with Figure 2a, the charge density data reveal that GdmSCN causes a shift in the charge density curve to lower V_{oc}. Because the overall trap density has not changed (Figure S6), the shift in charge versus V_{oc} is indicative of a more positive TiO_2 surface and a lower conduction band edge energy (V_{cb}). The downshift in V_{cb} is about 60 mV for N719 cells and 40 mV for D131 cells. Figure 5b shows that GdmSCN gives an electron lifetime about 4–5 times longer for N719, estimated for the average one sun charge density. (As the lifetime versus charge curves are neither straight nor parallel, it is not possible to give a single value for the increase in lifetime.) Given the V_{oc} ideality is 90 mV/decade for these cells, a 5-fold increase in recombination lifetime should give a 60 mV increase in V_{oc}. In the actual cells, this potential V_{oc} increase is exactly canceled by the 60 mV downshift in the conduction band, consistent with the $J-V$ curves (Table 1) where no change in V_{oc} is observed for N719.

In contrast, Figure 5b shows that Gdm^+ does not cause a change in recombination in the two D131 cells. This is consistent with the lack of competition between Gdm^+ and I_2 binding to D131, as seen in the binding measurements above. In the absence of a change in recombination, the ~40 mV downshift in the conduction band causes the ~30 mV decrease in the V_{oc} seen in the $J-V$ curves.

Consistent with Figure 2b, additional transient measurements on Z995 cells with and without Gdm^+ show the presence of Gdm^+ causes a factor 2–4 increase in the recombination lifetime (SI 7). The uncertainty is due to the change in collection efficiency with and without Gdm^+, which causes the position on the charge axis to be uncertain. Figure 2b also suggests that the Z995 catalyzes recombination relative to a bare TiO_2 film. As noted in Figure 3, Gdm^+ partially competes for the binding site of the iodine. This will reduce the catalysis of iodine reduction but apparently does not eliminate it. The binding constants of I_2 and Gdm^+ to Z995 were estimated by titration as shown in Figure S4. The binding constant of iodine to Z995 is relatively high (~3500 M^{-1}), compared to the binding constant of Gdm^+ (~400 M^{-1}). Only the very low concentration of free iodine in the cell allows Gdm^+ to occupy some of the binding sites. Consistent with this, increasing the concentration of GdmSCN to 1 M caused a 40 mV increase in photovoltage and some increase in photocurrent (Figure S14).

Comparison of the three dyes gives some insight into the mechanism by which Gdm^+ reduces recombination. Most interesting, the similar recombination change in N719 and Z995 suggests that the thiocyanates are not central to the effect. This is despite the fact that SCN^- binds iodine and Gdm^+ appears to remove this iodine. Our supposition at this point is that iodine bound to the SCN^- is too far from the TiO_2 surface to contribute significantly to the recombination flux. Since we do observe iodine binding to Z995, it must be binding to the pyridine or to the carboxylate. Comparing the structures of Z995 and N719, a similar binding site must be present on N719, as well. We will term this the R-site due to the red shift observed. By this logic, the small red shift caused by the iodine binding to the R-site on N719 is masked by the large blue shift due to iodine binding on the SCN^-. The R-site association with

dx.doi.org/10.1021/ja411560s | J. Am. Chem. Soc. 2014, 136, 7286–7294

the LUMO orbitals almost certainly means it is closer to the TiO_2 surface than the S terminals of the NCS groups. This explains why the R-site is more effective at catalysis of recombination. We have argued before that the surprisingly small blocking behavior of N719, relative to bare TiO_2, must be related to a balance between steric blocking of recombination at the surface and increased recombination by iodine binding near the surface. This latter can now be explained by the iodine binding to the R-site. We cannot yet explain why Z995 is so much more effective than N719 in catalyzing recombination.

We now consider the issue of an increase in injection efficiency caused by Gdm^+. Previous authors have reasoned that the downshift in conduction band energy, as seen in Figures 2a and 4a, is evidence enough to explain the increase in J_{sc} by an increase in injection. However, no publications have yet presented the absolute injection yield (e.g., by transient absorption). As mentioned above, our preliminary front/back IPCE analysis finds an increase in collection efficiency roughly similar to the increase in J_{sc} in Table 1. The collection efficiency increase is a result of the decrease in recombination. Additional transient absorption experiments (data not shown) have verified that an increase in collection efficiency occurs when GdmSCN is added to the electrolyte. At present, we have no need to include an increase in injection to explain the results for Z995 and N719. However, the small 5% increase in photocurrent for the D131 cells does not appear to arise by increased collection efficiency as recombination and transport are unchanged (Figures 5 and S9).

In Figure 2a, we see that GdmSCN causes only a minimal downshift in the conduction band energy (V_{cb}) on bare TiO_2. Thus, the larger shift when the dye is present results from Gdm^+ binding to the dye. If Gdm^+ binding occurs only on the outer surface of the dye molecule, such as the thiocyanates of N719, it would not likely increase the electrostatic driving force for injection. Injection occurs between the dye LUMO and the empty states on the TiO_2, and the LUMO of these dyes has already been designed to be close to the TiO_2 surface.

On the other hand, Gdm^+ is known to form large hydrogen-bonded assemblies with carbonate species in solids and solutions.[41,42] Gdm^+ may bind to dyes, such as N719, Z995, and D131, at the COO^- that is already attached to the TiO_2. We have noted above that the desorption of D131 in the presence of GdmSCN may be related to Gdm^+ binding at or near the attachment group. The additional positive charge between the bulk of the dye and the surface could increase the injection driving force. The localized positive charge might also lower any electrostatic barrier created by the excess negative charge of the carboxylate group. Either of these mechanisms may increase injection efficiency, explaining the increase in current seen with D131 when Gdm^+ is present. It is clear that additional investigations, including the determination of the binding site of Gdm^+ to the ruthenium dyes, will be required to determine if any changes in injection efficiency are occurring.

CONCLUSION

We have found that the presence of dye on the TiO_2 surface is essential for the addition of GdmSCN to the electrolyte to reduce the recombination and lower the conduction band energy. Using UV−vis spectroscopy, we have shown there is a binding interaction between Gdm^+ and the dyes N719, D131, and Z995. Moreover, Gdm^+ inhibits binding of iodine on the same molecule in the case of N719 and Z995. We propose that removal of bound iodine close to the TiO_2 surface accounts for the reduced recombination in the presence of GdmSCN. This is confirmed by the fact that D131, for which Gdm^+ does not inhibit iodine binding, shows no decrease in recombination. In combination with our earlier papers on dye−iodine binding, we conclude that the interaction of electrolyte additives with the TiO_2 has been overemphasized, and that interaction with the dye layer is at least equally likely to be the mechanism by which such additives act. We speculate that this finding might include the effects of Li^+ and even possibly Cheno, subjects for further study in the future.

ASSOCIATED CONTENT

Supporting Information

Additional tables and figures as described in the paper. This material is available free of charge via the Internet at http://pubs.acs.org.

AUTHOR INFORMATION

Corresponding Author

b.oregan@imperial.ac.uk

Notes

The authors declare no competing financial interest.

ACKNOWLEDGMENTS

Financial support for this work was supplied by UK EPSRC project APEX (EP/H040218/1), the UK EPSRC project SPECIFIC (EP/I019278/1), the EU FP7 project SMARTOP (ref#265769), and the UK TSB project '"Water based electrolytes"' (TS/I001832/1).

REFERENCES

(1) Dudkowski, S. J.; Grossweiner, L. I. *J. Opt. Soc. Am.* **1964**, *54*, 486.
(2) Namba, S.; Hishiki, Y. *J. Phys. Chem.* **1965**, *69*, 774.
(3) Gerischer, H.; Michel-Beyerle, M. E.; Rebentrost, F.; Tributsch, H. *Electrochim. Acta* **1968**, *13*, 1509.
(4) Memming, R.; Tributsch, H. *J. Phys. Chem.* **1971**, *75*, 562.
(5) Morrison, S. R. *Electrochemistry at Semiconductor and Oxidized Metal Electrodes*; Plenum Press: New York, 1980.
(6) Gerischer, H. *Faraday Discuss. Chem. Soc.* **1974**, *58*, 219.
(7) Wang, P.; Zakeeruddin, S. M.; Humphry-Baker, R.; Moser, J. E.; Grätzel, M. *Adv. Mater.* **2003**, *15*, 2101.
(8) Huang, S. Y.; Schlichthörl, G.; Nozik, A. J.; Grätzel, M.; Frank, A. J. *J. Phys. Chem. B* **1997**, *101*, 2576.
(9) Kay, A.; Graetzel, M. *J. Phys. Chem.* **1993**, *97*, 6272.
(10) Nazeeruddin, M. K.; Kay, A.; Rodicio, I.; Humphry-Baker, R.; Mueller, E.; Liska, P.; Vlachopoulos, N.; Graetzel, M. *J. Am. Chem. Soc.* **1993**, *115*, 6382.
(11) Boschloo, G.; Häggman, L.; Hagfeldt, A. *J. Phys. Chem. B* **2006**, *110*, 13144.
(12) Wang, M.; Li, X.; Lin, H.; Pechy, P.; Zakeeruddin, S. M.; Gratzel, M. *Dalton Trans.* **2009**, 10015.
(13) Allegrucci, A.; Lewcenko, N. A.; Mozer, A. J.; Dennany, L.; Wagner, P.; Officer, D. L.; Sunahara, K.; Mori, S.; Spiccia, L. *Energy Environ. Sci.* **2009**, *2*, 1069.
(14) Kopidakis, N.; Neale, N. R.; Frank, A. J. *J. Phys. Chem. B* **2006**, *110*, 12485.
(15) Mosconi, E.; Yum, J.-H.; Kessler, F.; Gómez García, C. J.; Zuccaccia, C.; Cinti, A.; Nazeeruddin, M. K.; Grätzel, M.; De Angelis, F. *J. Am. Chem. Soc.* **2012**, *134*, 19438.
(16) O'Regan, B. C.; Walley, K.; Juozapavicius, M.; Anderson, A.; Matar, F.; Ghaddar, T.; Zakeeruddin, S. M.; Klein, C. D.; Durrant, J. R. *J. Am. Chem. Soc.* **2009**, *131*, 3541.
(17) Pastore, M.; Mosconi, E.; De Angelis, F. *J. Phys. Chem. C* **2012**, *116*, 5965.

(18) Li, X.; Reynal, A.; Barnes, P.; Humphry-Baker, R.; Zakeeruddin, S. M.; De Angelis, F.; O'Regan, B. C. *Phys. Chem. Chem. Phys.* **2012**, *14*, 15421.
(19) Planells, M.; Pelleja, L.; Clifford, J. N.; Pastore, M.; De Angelis, F.; Lopez, N.; Marder, S. R.; Palomares, E. *Energy Environ. Sci.* **2011**, *4*, 1820.
(20) Asaduzzaman, A. M.; Chappellaz, G. A. G.; Schreckenbach, G. *J. Comput. Chem.* **2012**, *33*, 2492.
(21) Richards, C. E.; Anderson, A. Y.; Martiniani, S.; Law, C.; O'Regan, B. C. *J. Phys. Chem. Lett.* **2012**, *3*, 1980.
(22) O'Regan, B.; Xiaoe, L.; Ghaddar, T. *Energy Environ. Sci.* **2012**, *5*, 7203.
(23) Jeong, N. C.; Son, H.-J.; Prasittichai, C.; Lee, C. Y.; Jensen, R. A.; Farha, O. K.; Hupp, J. T. *J. Am. Chem. Soc.* **2012**, *134*, 19820.
(24) Hagfeldt, A.; Boschloo, G.; Sun, L.; Kloo, L.; Pettersson, H. *Chem. Rev.* **2010**, *110*, 6595.
(25) Grätzel, M. *J. Photochem. Photobiol., C* **2003**, *4*, 145.
(26) Grätzel, M. *J. Photochem. Photobiol., A* **2004**, *164*, 3.
(27) Wang, P.; Klein, C.; Humphry-Baker, R.; Zakeeruddin, S. M.; Gratzel, M. *Appl. Phys. Lett.* **2005**, *86*, 123508.
(28) Yu, Z.; Gorlov, M.; Boschloo, G.; Kloo, L. *J. Phys. Chem. C* **2010**, *114*, 22330.
(29) Miettunen, K.; Barnes, P. R. F.; Li, X.; Law, C.; O'Regan, B. C. *J. Electroanal. Chem.* **2012**, *677*−*680*, 41.
(30) O'Regan, B. C. www3.imperial.ac.uk/people/b.oregan.
(31) O'Regan, B. C.; Lenzmann, F. *J. Phys. Chem. B* **2004**, *108*, 4342.
(32) O'Regan, B. C.; Durrant, J. R.; Sommeling, P. M.; Bakker, N. J. *J. Phys. Chem. C* **2007**, *111*, 14001.
(33) Barnes, P. R. F.; Anderson, A. Y.; Juozapavicius, M.; Liu, L.; Li, X.; Palomares, E.; Forneli, A.; O'Regan, B. C. *Phys. Chem. Chem. Phys.* **2011**, *13*, 3547.
(34) Barnes, P. R. F.; Anderson, A. Y.; Koops, S. E.; Durrant, J. R.; O'Regan, B. C. *J. Phys. Chem. C* **2009**, *113*, 1126.
(35) Zhang, C.; Huang, Y.; Huo, Z.; Chen, S.; Dai, S. *J. Phys. Chem. C* **2009**, *113*, 21779.
(36) Koops, S. E.; O'Regan, B. C.; Barnes, P. R. F.; Durrant, J. R. *J. Am. Chem. Soc.* **2009**, *131*, 4808.
(37) Liu, Y.; Hagfeldt, A.; Xiao, X.-R.; Lindquist, S.-E. *Sol. Energy Mater. Sol. Cells* **1998**, *55*, 267.
(38) Jose, R.; Kumar, A.; Thavasi, V.; Fujihara, K.; Uchida, S.; Ramakrishna, S. *Appl. Phys. Lett.* **2008**, *93*, 023125.
(39) Le Bahers, T.; Pauporte, T.; Scalmani, G.; Adamo, C.; Ciofini, I. *Phys. Chem. Chem. Phys.* **2009**, *11*, 11276.
(40) Nazeeruddin, M. K.; Humphry-Baker, R.; Liska, P.; Grätzel, M. *J. Phys. Chem. B* **2003**, *107*, 8981.
(41) Mason, P. E.; Neilson, G. W.; Kline, S. R.; Dempsey, C. E.; Brady, J. W. *J. Phys. Chem. B* **2006**, *110*, 13477.
(42) Mak, T. C. W.; Xue, F. *J. Am. Chem. Soc.* **2000**, *122*, 9860.